Translational Science

Cancer Research

Circulating Tumor Cells Undergoing EMT Provide a Metric for Diagnosis and Prognosis of Patients with Hepatocellular Carcinoma

Lu-Nan Qi[1,2,3], Bang-De Xiang[1,2,3], Fei-Xiang Wu[1,2,3], Jia-Zhou Ye[1], Jian-Hong Zhong[1], Yan-Yan Wang[1], Yuan-Yuan Chen[4], Zu-Shun Chen[1], Liang Ma[1], Jie Chen[1], Wen-Feng Gong[1], Ze-Guang Han[5], Yan Lu[6], Jin-Jie Shang[7], and Le-Qun Li[1,2,3]

Abstract

To clarify the significance of circulating tumor cells (CTC) undergoing epithelial–mesenchymal transition (EMT) in patients with hepatocellular carcinoma (HCC), we used an advanced CanPatrol CTC-enrichment technique and *in situ* hybridization to enrich and classify CTC from blood samples. One hundred and one of 112 (90.18%) patients with HCC were CTC positive, even with early-stage disease. CTCs were also detected in 2 of 12 patients with hepatitis B virus (HBV), both of whom had small HCC tumors detected within 5 months. CTC count $\geq$16 and mesenchymal–CTC (M-CTC) percentage $\geq$2% prior to resection were significantly associated with early recurrence, multi-intrahepatic recurrence, and lung metastasis. Postoperative CTC monitoring in 10 patients found that most had an increased CTC count and M-CTC percentage before clinically detectable recurrence nodules appeared. Analysis of HCC with high CTC count and high M-CTC percentage identified 67 differentially expressed cancer-related genes involved in cancer-related biological pathways (e.g., cell adhesion and migration, tumor angiogenesis, and apoptosis). One of the identified genes, BCAT1, was significantly upregulated, and knockdown in Hepg2, Hep3B, and Huh7 cells reduced cell proliferation, migration, and invasion while promoting apoptosis. A concomitant increase in epithelial marker expression (EpCAM and E-cadherin) and reduced mesenchymal marker expression (vimentin and Twist) suggest that BCAT1 may trigger the EMT process. Overall, CTCs were highly correlated with HCC characteristics, representing a novel marker for early diagnosis and a prognostic factor for early recurrence. BCAT1 overexpression may induce CTC release by triggering EMT and may be an important biomarker of HCC metastasis.

Significance: In liver cancer, CTC examination may represent an important "liquid biopsy" tool to detect both early disease and recurrent or metastatic disease, providing cues for early intervention or adjuvant therapy. *Cancer Res; 78(16); 4731–44. ©2018 AACR.*

Introduction

Hepatocellular carcinoma (HCC) is a major health problem worldwide, with more than 700, 000 cases diagnosed annually (1). Despite improvements in surveillance and treatment, the prognosis remains poor due to the high incidence of recurrence and metastasis. Moreover, conventional liver imaging for HCC diagnosis and staging are somewhat imprecise and can result in underestimation of disease stage. Microvascular invasion and metastasis are often identified at resection and are associated with significantly poorer prognosis (2).

Circulating tumor cells (CTC) originating from solid tumors are related to hematogeneous metastatic spread to distant sites; therefore, CTC analysis has clinical relevance as a biomarker to noninvasively monitor cancer progression and guide therapy (2–8). In patients with early-stage breast cancer, CTC levels correlated with stage, lymph node status, and survival (9). Patients with CTC-positive HCC have a higher risk of recurrence and shorter recurrence-free survival (10). CTCs disseminate from primary tumors by undergoing phenotypic changes that allow them to penetrate blood vessels, including epithelial–mesenchymal transition (EMT; refs. 11–13). Therefore, CTCs may be classified into three types: epithelial, mesenchymal, and epithelial/mesenchymal hybrids. In HCC, Nel and colleagues (14) showed that a change in the epithelial-to-mesenchymal–CTC ratio was associated with progression.

Although techniques for CTC isolation and characterization based on their physical properties or cell surface antigen expression have been reported (6, 7, 15, 16), epithelial antigen–based

[1]Department of Hepatobiliary Surgery, Affiliated Tumor Hospital of Guangxi Medical University, Nanning, Guangxi Province, China. [2]Guangxi Liver Cancer Diagnosis and Treatment Engineering and Technology research center, Nanning, Guangxi Province, China. [3]Key Laboratory of Early Prevention and Treatment for Regional High Frequency Tumor, Ministry of Education, Nanning, Guangxi Province, China. [4]Department of Ultrasound, First Affiliated Hospital of Guangxi Medical University, Nanning, Guangxi Province, China. [5]China National Human Genome Center at Shanghai, Shanghai, Shanghai City, China. [6]SurExam Bio-Tech, Guangzhou Technology Innovation Base, Science City, Guangzhou, Guangdong Province, China. [7]Jiangsu Key Laboratory for Microbes and Functional Genomics, College of Life Sciences, Nanjing Normal University, Nanjing, Jiangsu Province, China.

Note: Supplementary data for this article are available at Cancer Research Online (http://cancerres.aacrjournals.org/).

L.-N. Qi, B.-D. Xiang, and F.-X. Wu contributed equally to this article.

Corresponding Author: Le-Qun Li, Affiliated Tumor Hospital of Guangxi Medical, Department of Hepatobiliary Surgery, Affiliated Tumor Hospital of Guangxi Medical University, Nanning, Guangxi Province, China, Nanning, 530021, China. Phone: 0771-5310045; E-mail: lequnlibbcd66@mcatom.cn

doi: 10.1158/0008-5472.CAN-17-2459

approaches may fail to detect some aggressive CTC subpopulations that may have undergone EMT. Recently, an optimized CanPatrol CTC-enrichment technique based on RNA *in situ* hybridization (RNA-ISH) has been reported. This technique uses epithelial and mesenchymal markers (e.g., EpCAM, E-cadherin, CK8/18/19, vimentin, and Twist) to characterize and classify CTCs into all three CTC subpopulations. Compared with other techniques, CanPatrol CTC-enrichment permits identification and classification of all CTC subpopulations with high collective efficiency. This technique has been used in a range of carcinomas (8, 17–20).

Because few studies have analyzed CTCs undergoing EMT in HCC, the present study used CanPatrol CTC enrichment with an RNA-ISH assay to enrich and classify CTCs from patients with HCC. We also explored the relationship between the CTC subpopulations and patient characteristics and outcomes. Gene expression analysis was performed to identify genes that may contribute to CTC release to provide additional insight into the genetic mechanisms of CTCs.

Patients and Methods

Patient samples

From March 2014 to August 2016, a total of 112 patients with HCC treated with R0 resection at the Tumor Hospital of Guangxi Medical University Nanning, Guangxi Province, China, were enrolled. The inclusion criteria were as follows: (i) Child–Pugh A stage and PST score 0–1; (ii) definitive pathological diagnosis of HCC based on World Health Organization criteria (21); (iii) R0 resection defined as complete macroscopic removal of the tumor, resection margins negative, and no detectable intrahepatic and extrahepatic metastasis lesions remaining; (iv) no prior anticancer treatment. Tumor stage was determined according to the Barcelona Clinic Liver Cancer (BCLC) staging system, and tumor differentiation was defined according to the Edmondson grading system (22). In addition, 20 healthy donors and 12 patients with hepatitis B virus (HBV) were enrolled as controls. Endpoint of follow-up was May 31, 2017. This study was conducted in accordance with the Declaration of Helsinki guidelines, and the protocol of this trial was approved by the ethics committee of the Tumor Hospital of Guangxi Medical University. All patients and healthy volunteers provided written informed consents.

Isolation of CTCs by CanPatrol system and tricolor RNA-ISH assay

The CanPatrol system was used to isolate CTCs as previously described (Fig. 1A; refs. 17, 20, 23, 24). The time points for blood collection were 1 or 2 days before resection, and a median of 9 days (range, 8–10 days) after resection. Peripheral blood samples (5 mL, anticoagulated with EDTA) were collected after discarding the first 2 mL to avoid potential skin cell contamination from the venipuncture (19). The filtration system included a filtration tube containing a membrane with 8-μm diameter pores (Sur Exam), a manifold vacuum plate with valve settings (SurExam), an E-Z96 vacuum manifold (Omega), and a vacuum pump (Auto Science). Before filtration, red blood cell lysis buffer was used to remove erythrocytes, and the cells were resuspended in PBS with 4% formaldehyde (Sigma) for 5 minutes. The pumping pressure was 0.08 MPa (19).

RNA-ISH was used to detect the following target sequences: CD45 (leukocyte biomarker), EpCAM, CK8/18/19 (epithelial biomarkers), vimentin, and Twist (mesenchymal biomarkers). The assay was performed in a 24-well plate (Corning), and the cells on the membrane were treated with a protease (Qiagen) before hybridization with a capture probe specific for all genes above (Supplementary Table S1). Hybridization was performed as previously described (8, 17–19). We used 4′,6-diamidino-2-phenylindole (DAPI) to stain the nuclei, and the cells were analyzed with a fluorescent microscope.

DNA extraction and purification and analysis of the p53 gene R249S mutation

Genomic DNA was extracted using the DNeasy Tissue kit (Qiagen) according to the manufacturer's recommendation. enomic DNA extraction from the CTCs was also performed. Briefly, the membrane was mounted with 1% agarose on a standard size slide, and target cells underwent laser microdissection using a PALM MicroBeam (Zeiss). Target cells were incubated in 15 μL of lysis buffer (10 mmol/L Tris–HCl, pH8 and 200 mg/mL proteinase K) at 52°C overnight. Following centrifugation at 10,000 × *g* for 5 minutes, the cell lysate underwent whole genome amplification with a GenomePlex Single Cell Whole Genome Amplification Kit (Sigma-Aldrich).

Exon 7 of *p53* was amplified using the following primers under standard cycling conditions: 5′-cttgccacaggtctccccaa-3′ and 5′-aggggtcagcggcaagcaga-3′ (237 bp). Purified PCR products were sequenced to evaluate the presence of the $AGG^{Arg}\rightarrow AGT^{Ser}$ or $AGG^{Arg}\rightarrow AGC^{Ser}$ mutation at codon 249.

RNA extraction and purification, array hybridization, and data acquisition

Total RNA was extracted using a Takara RNAiso Plus Kit (Cat# 9109, Takara Bio Inc.) following the manufacturer's instructions. Total RNA was further purified using an RNeasy mini kit (Cat# 74106, QIAGEN) and RNase-Free DNase Set (Cat# 79254, QIAGEN). Array hybridization and washing were performed using a GeneChip Hybridization, Wash and Stain Kit (Cat #900720, Affymetrix) in Hybridization Oven 645 (Cat# 00-0331-220V, Affymetrix) and Fluidics Station 450 (Cat# 00-0079, Affymetrix, Thermo Fisher Scientific) following the manufacturer's instructions. Slides were scanned using a GeneChip Scanner 3000 (Cat# 00-00212, Affymetrix, Thermo Fisher Scientific) and Command Console Software 4.0 (Affymetrix, Thermo Fisher Scientific) with default settings. Raw data were normalized using a RMA algorithm, Affy packages in R.

Semiquantitative RT-PCR, real-time quantitative PCR, and Western blotting

cDNA was synthesized from total RNA with the RevertAid First Strand cDNA Synthesis Kit (Thermo Fisher Scientific) according to the manufacturer's instructions. cDNA amplification was performed using standard conditions, and the primer sequences for RT-PCR and quantitative (q)PCR are listed in Supplementary Table S2. For qPCR, relative expression of the target gene was compared with the internal control gene using the comparative $-\Delta\Delta Ct$ method.

For Western blot analysis, total proteins were extracted in RIPA lysis buffer. Following 10% SDS–PAGE, the proteins were transferred onto a PVDF membrane, which were blocked in 5% nonfat milk. After incubation with primary antibodies (anti-BCAT1, anti-EpCAM, anti-E-cadherin, anti-Twist, anti-vimentin, and anti-β-actin antibodies; Abcam) overnight at 4°C, the membranes

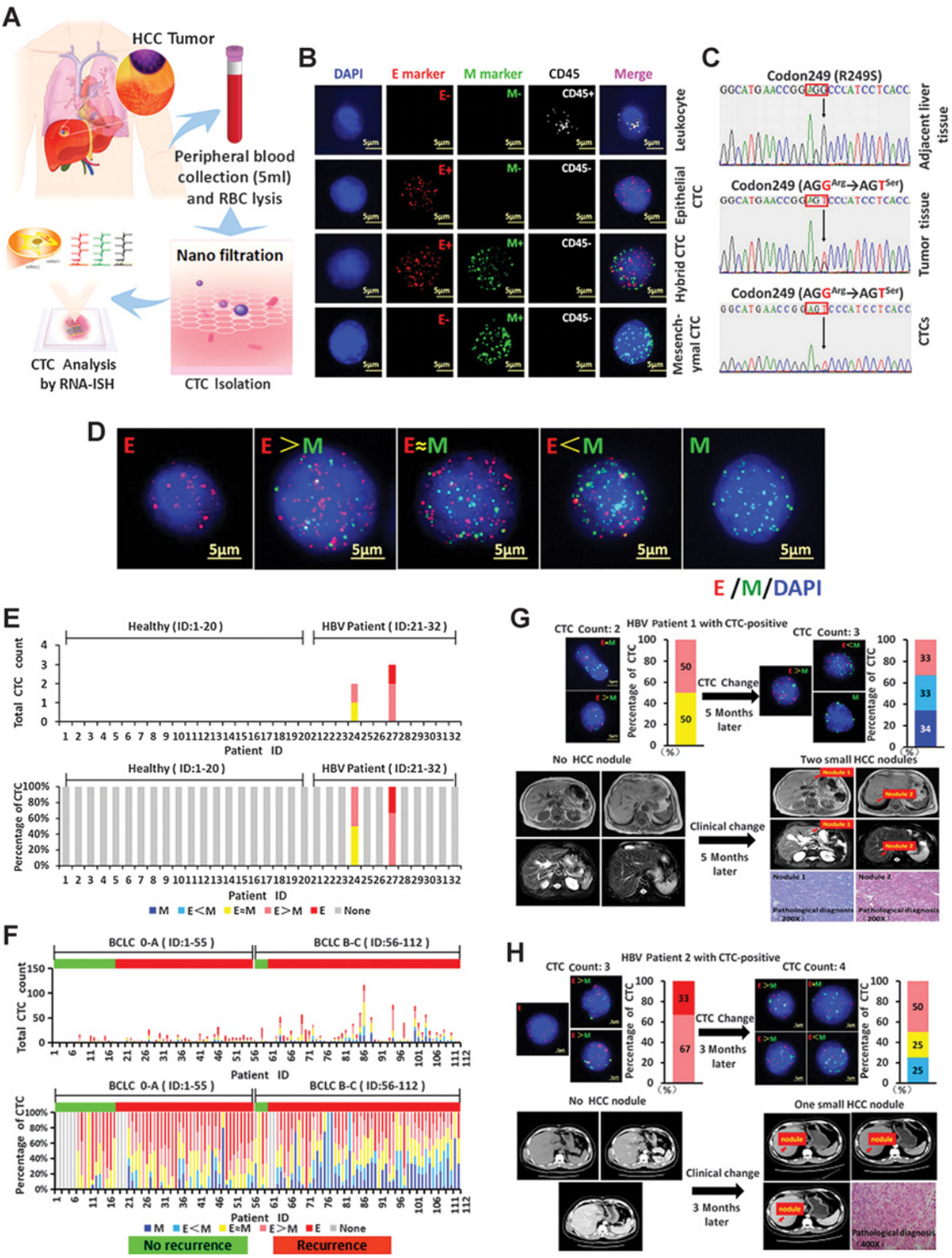

Figure 1.

CTC isolation and RNA-ISH analysis of blood samples from patients with HCC, patients with HBV, and healthy donors. **A,** Process of CTC isolation and detection by CanPatrol CTC enrichment and ISH. **B,** Detection and classification of CTCs using EMT markers. Leukocytes were stained for CD45 (white fluorescence). CTCs were stained for epithelial markers (EpCAM and CK8/18/19, red fluorescence) and mesenchymal markers (vimentin and Twist, green fluorescence). The cells were analyzed using a 100× objective. **C,** Representative image of *p53* gene mutation detection showed the same R249S mutation in the primary tumor and CTCs, but not in nontumor liver tissues, confirming that the CTCs originated from the primary tumor. **D,** Representative images of five types of CTCs isolated from patients with HCC based on RNA-ISH staining of epithelial (red fluorescence) and mesenchymal (green fluorescence) markers. **E,** Total CTC counts (top) and percentage of each CTC type (bottom) in the healthy controls and patients with HBV. Two patients with HBV had a CTC-positive blood sample. **F,** Total CTC counts (top) and percentage of each CTC type (bottom) in patients with BCLC 0–A and B–C stage HCC. **G** and **H,** Images of both patients with HBV who had a CTC-positive blood sample without any detectable nodes at that time. At 3- and 5-month follow-up, small, detectable HCC tumors were observed in the liver by CT and MRI.

were incubated with secondary antibodies for 2 hours at 37°C. Proteins were visualized with ECL Western blotting detection reagents (Pierce Thermo Scientific), and the bands were quantified using QUANTITY ONE software (Bio-Rad).

BCAT1 knockdowns in Hepg2, Hep3B, and Huh7 cells

Two short-hairpin RNAs (shRNA) targeting the BCAT1 sequence (sh1:5′-ggaaattggttgactatta-3′; sh2: 5′-gggaacagagtgaga-gaga-3′) were designed using the siRNA Ambion Target Finder software (http://www.ambion.com/techlib/misc/siRNA_finder.html). Three HCC cell lines with high or moderate BCAT1 expression (Hepg2, Hep3B, and Huh7) were obtained from the ATCC (Hepg2 and Hep3B) and Japanese Collection of Research Bioresources (Huh7) on 2015. These cells were used within 8 passages and further authenticated by short-tandem repeat analysis on 2017. All three underwent *Mycoplasma* testing on 2017 by PCR by Shanghai Biowing Biotechnology Co. Ltd. All three cell lines were stably transfected with the shRNA-BCAT1 plasmid using the ExGen500 transfection reagent (Fermentas), according to the manufacturer's instructions. Cells were cultured for 2 weeks in selection medium containing 0.5 μg/mL puromycin (Wisent), and BCAT1 expression was evaluated by Western blot analysis. In addition, cells with the stably transfected BCAT1-sh1-rescue clone were used as controls.

Cell proliferation analysis

Cell proliferation was determined using the CCK-8 Kit (Dojindo Laboratories) according to the manufacturer's protocols. At 1, 2, 3, 4, and 5 days, cells were stained with 10 μL of CCK-8 reagent at 37°C for 2 hours, and absorbance was measured at 450 nm. All assays were performed in quadruplicate.

Analysis of apoptosis by flow cytometry

At 48 hours following transfection with shBCAT1 or shBCAT1-rescue, cells were harvested and washed twice with ice-cold PBS. The cells were suspended in the Annexin V–binding buffer to a final concentration of 10^6 cells/mL and incubated with AlexaFluor647 Annexin V (Biolegend) for 15 minutes at 4°C in the dark, after which, propidium iodide (Sigma) was added. Samples were immediately analyzed by flow cytometry using a BD FACSCantoll (BD Biosciences).

Cell migration and invasion assays

For the invasion assay, 8-μm pore Transwell inserts coated with Matrigel in cold serum-free media were seeded with 5×10^4 cells/well and incubated for 48 hours. Noninvasive cells on the upper surface of the filter were removed by wiping with a cotton swab, and the cells that migrated through the membrane and stuck to the lower surface of the membrane were fixed with 10% paraformaldehyde and stained with 0.1% hexamethylpararosaniline for 30 minutes. The number of cells was counted in five predetermined fields under a microscope. Data were expressed as the average number of cells migrating through the filters. The migration assay was similar to the Matrigel invasion assay with the exception of the presence of Matrigel, an 18-hour incubation, and methanol fixation.

Statistical analysis

Patient characteristics were shown as count and percentages for categorical data, and mean ± standard deviation (SD) with ranges (minimum, maximum) for continuous data. Comparisons among groups were analyzed using Kruskall–Wallis tests with pair-wise comparisons or Mann–Whitney *U* test if the data did were not normally distributed. Patient characteristics associated with HCC recurrence were determined by univariate and multivariate Cox-regression analyses. Significant variables in the univariate Cox-regression analysis ($P < 0.05$) were selected for multivariate Cox-regression analysis with a backward stepwise selection (Wald). Receiver operating characteristic (ROC) curve analysis with maximal Youden index values was applied to identify best cutoff values for preoperative CTC count and mesenchymal–CTC percentage for recurrence. The association of early recurrence with CTC count and mesenchymal–CTC percentage (subgrouped by the best cutoff values) was detected using Pearson χ^2 tests or Fisher exact tests if any cell number was <5. A Kaplan–Meier curve with a log-rank test was performed to identify associations between postoperative tumor-free survival time with changes in total CTC count or M-CTC percentage. All statistical assessments were two-tailed, and $P < 0.05$ were considered statistically significant. All statistical analyses were performed with IBM SPSS statistical software version 22 for Windows (IBM). Scatter plots were graphed using GraphPrism Version 6.01 (GraphPad Software).

Results

Patient characteristics

Patient characteristics are summarized in Supplementary Table S3. A total of 112 patients with HCC with R0 resection (92 males and 20 females) with a mean age of 47.1 years (range, 20–72 years) were enrolled. Among the patients, 11 (9.8%) were BCLC stage 0, 44 (39.3%) BCLC stage A, 24 (21.4%) BCLC stage B, and 33 (29.5%) BCLC stage C.

Identification of CTC subpopulations in the blood of all patients and healthy volunteers

Using the CanPatrol CTC-enrichment technique, many CTCs were detected in the blood samples. As shown in Fig. 1B, the red and green fluorescent signals represented epithelial and mesenchymal gene expression, respectively. The white fluorescent signal represented *CD45* gene expression (i.e., leukocyte marker).

In order to verify that these CTCs were from the primary HCC and not other tissues, we analyzed 5 patients who had the R249S mutation (4 with an $AGG^{Arg} \rightarrow AGT^{Ser}$ mutation and one with an $AGG^{Arg} \rightarrow AGC^{Ser}$ mutation) in the *p53* gene in the primary tumor but not in nontumor liver tissues. We detected the same R249S mutation in the DNA of these CTCs, confirming the CTCs originated from the primary tumor (Fig. 1C; Supplementary Fig. S1).

Analysis of the CTCs by RNA-ISH revealed five subpopulations: (i) epithelial CTCs (E-CTC), (ii) epithelial predominant hybrid CTCs (E>M-CTC), (iii) epithelial/mesenchymal hybrid CTCs (E≈M-CTC), (iv) mesenchymal predominant hybrid CTCs (M>E-CTC), and (v) mesenchymal CTCs (M-CTC; Fig. 1D). CTCs were detected in 101 of 112 (90.18%) patients with HCC. In addition, 2 of 12 (16.67%) patients with HBV had CTCs, but none were found in 20 healthy donors (Fig. 1E and F). Interestingly, both patients with CTC-positive HBV were followed every 1–2 months, and very small HCC nodules were detected at the 3- and 5-month follow-up, respectively (Fig. 1G and H). Because of the early detection, both patients have received more timely and effective treatment.

Prognostic significance of CTC counts and subtypes before surgical resection

We first analyzed the correlation between CTCs and BCLC stage. The positive rate of CTCs was 83.6% (46/55) and 96.5% (55/57) in patients with BCLC stage 0–A and stage B–C tumors, respectively (Fig. 1F). The median CTC count in patients with advanced HCC (stages B–C) was significantly higher than in patients with early-stage HCC (stages 0–A; $P < 0.001$; Fig. 2A). In addition, the median proportion of M-CTCs was greater in patients with advanced HCC as compared with early-stage HCC

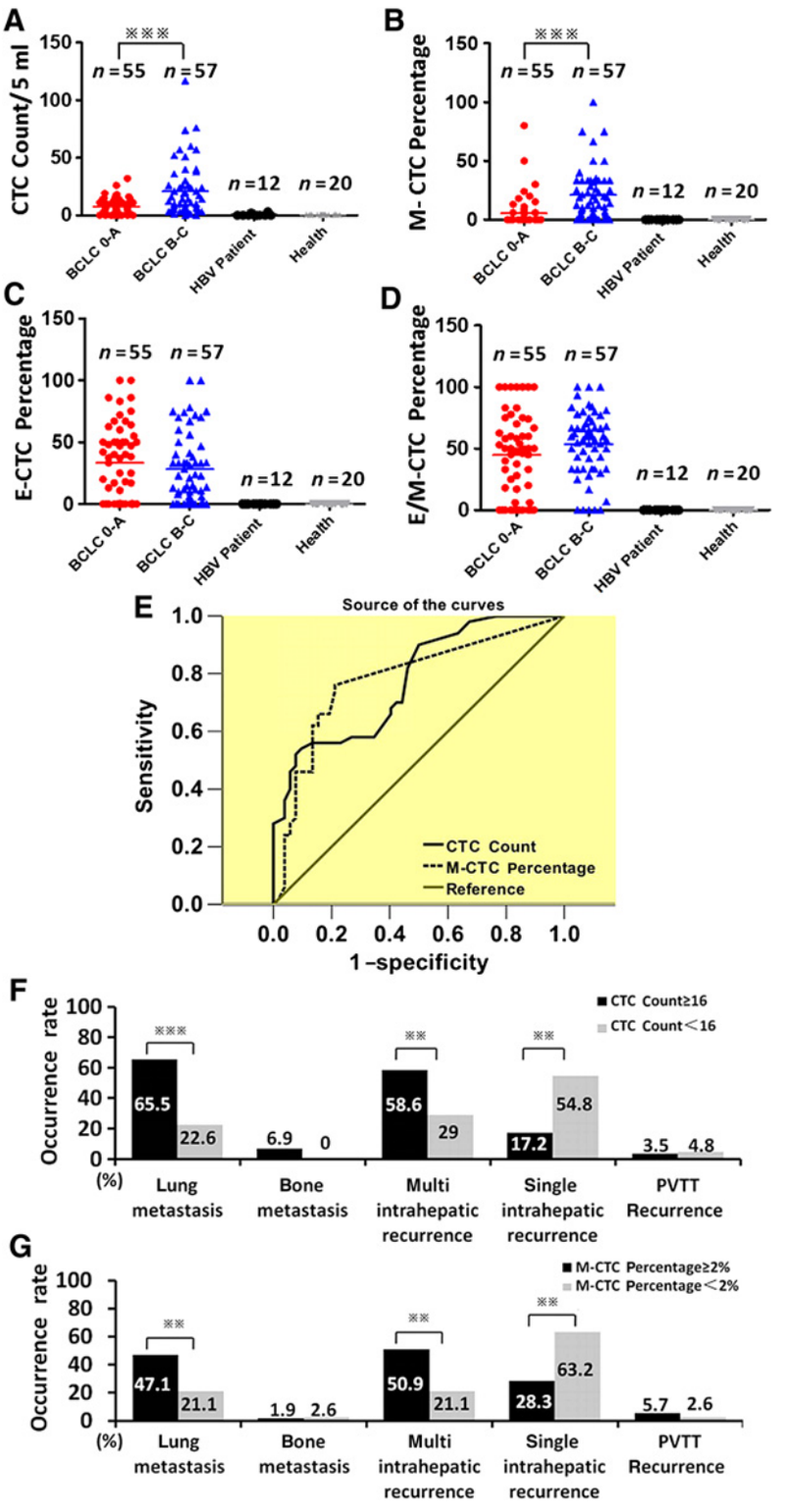

Figure 2.

Prognostic significance of CTC counts and subtypes before surgical resection. **A–D,** Total CTC count (**A**) and percentage of M-CTCs (**B**), E-CTCs (**C**), and E/M-CTCs (**D**) among patients with HCC with early- and late-stage tumors, patients with HBV, and healthy controls. Both the median CTC count and M-CTC percentage in patients with advanced HCC (stages B–C) were significantly higher than that in patients with early-stage HCC (stage 0–A). **, $P < 0.05$; ***, $P < 0.001$. **E,** ROC curves for total CTC count and M-CTC percentage. The best cutoff for each was 16 for CTC count and 2% for M-CTC percentage according to the maximization of Younden index from the ROC curve analysis. **F** and **G,** The incidence of recurrence at different five sites in 91 patients with HCC by CTC count (**F**) or M-CTC percentage (**G**). **, $P < 0.05$; ***, $P < 0.001$.

Table 1. Univariate and multivariate Cox-regression analysis of preoperative patient characteristics associated with HCC recurrence ($n = 112$)

Characteristics		Univariate		Multivariate	
		HR (95% CI)	P	HR (95% CI)	P
Age	≥45 vs. <45 years	0.904 (0.587–1.392)	0.904		
Sex	Female vs. male	1.275 (0.748–2.17)	0.372		
HBsAg	Positive vs. negative	0.990 (0.539–1.819)			
HBV-DNA	≥500 vs. <500	0.955 (0.594–1.535)			
AFP level	≥400 vs. <400 ng/mL	2.425 (1.552–3.789)	<0.001	1.583 (0.929–2.696)	0.091
Liver cirrhosis	Positive vs. Negative	1.608 (1.053–2.455)	0.028	1.323 (0.816–2.145)	0.256
Tumor size[a]	≥5 vs. <5 cm	2.289 (1.379–3.799)	0.001	1.206 (0.651–2.232)	0.552
Edmondson grade[a]	Poorly vs. Well differentiated	1.419 (0.903–2.230)	0.130		
BCLC stage	B-C vs. 0-A	4.114 (2.616–6.470)	<0.001	1.799 (0.763–4.244)	0.180
Node number	Multi (≥2 nodes) vs. single	2.841 (1.851–4.361)	<0.001	1.223 (0.607–2.466)	0.574
MVI	Positive vs. negative	2.588 (1.610–4.160)	<0.001	1.477 (0.812–2.686)	0.201
PVTT	Positive vs. negative	4.490 (2.749–7.333)	<0.001	0.950 (0.461–1.959)	0.890
Tumor capsule[a]	Negative vs. positive	4.520 (2.861–7.139)	<0.001	2.332 (1.310–4.150)	0.004
LN metastasis	Positive vs. negative	2.448 (0.596–10.045)	0.214		
CTC count		1.038 (1.027–1.050)	<0.001	1.021 (1.007–1.036)	0.003
M-CTC percentage		1.019 (1.010–1.027)	<0.001	1.019 (1.006–1.032)	0.003
M>E-CTC percentage		1.021 (1.009–1.034)	0.001	1.004 (0.986–1.022)	0.661
M≈E-CTC percentage		1.000 (0.989–1.010)	0.925		
M<E-CTC percentage		1.000 (0.990–1.010)	0.998		
E-CTC percentage		1.000 (0.993–1.007)	0.970		

Abbreviations: HR, hazard ratio; CI, confidence intervals; HBV, hepatitis B virus; AFP, α-fetoprotein; MVI, microvascular invasion; PVTT, portal vein tumor thrombus; LN, lymph node; CTC, circulating tumor cell.

[a]If the patient had multiple nodes, the largest one was indicated.

($P < 0.001$; Fig. 2B). No differences in the median proportion of E-CTCs or E/M-CTCs were detected between patients with early- or late-stage disease (Fig. 2C and D).

During the study period, 91 (81.2%) patients had recurrence, with a mean time for recurrence of 9.5 months. The recurrence rate was 69.1% (38/55) and 92.9% (53/57) in patients with BCLC stage 0–A and stage B–C, respectively. Table 1 shows univariate and multivariate Cox-regression analyses of preoperative factors associated with postoperative HCC recurrence. Univariate analysis showed that postoperative recurrence might be associated with AFP level, liver cirrhosis, tumor size, BCLC stage, node number, microvascular invasion (MVI), portal vein tumor thrombus (PVTT), tumor capsule, CTC count, M-CTC percentage, and M>E-CTC percentage (all, $P < 0.05$). Multivariate analysis revealed that BCLC stage B–C, positive MVI, negative tumor capsule, and increased CTC count and M-CTC percentage were associated with greater risk of postoperative HCC recurrence (all, $P < 0.05$).

We next analyzed whether CTC count and M-CTC percentage were predictors of early recurrence (recurrence within 6 months) after surgery. Forty-seven patients (51.6%) had early recurrence, and 44 (48.4%) had late recurrence. ROC curve analysis showed area under the curve values of 0.74 (95% CI, 0.64–0.84; $P < 0.001$) and 0.75 (95% CI, 0.66–0.84; $P < 0.001$) for CTC count and M-CTC percentage, respectively (Fig. 2E). The best cutoff was 16 for CTC count and 2% for M-CTC percentage according to maximization of the Younden index (CTC count: sensitivity = 55.3% and specificity = 92.3%; M-CTC percentage: sensitivity = 80.9% and specificity = 69.2%).

For early recurrence patients, 34.0%, 21.3%, and 14.9% were classified as multi-intrahepatic + lung, lung only, and multi-intrahepatic, respectively (Table S4). For those with late recurrence, the majority was classified as single-intrahepatic and multi-intrahepatic recurrence (70.5% and 22.7%, respectively; Supplementary Table S4). In addition, patients with CTC count ≥16 had significantly higher multi-intrahepatic and lung-only recurrence as compared with those with CTC count <16 (multi-intrahepatic: 58.6% vs. 29.0%, $P = 0.007$; lung only: 65.5% vs. 22.6%, $P < 0.001$; Fig. 2F). In contrast, patients with CTC count <16 had greater single-intrahepatic recurrence than those with CTC count ≥16 (54.8% vs.17.2%, $P = 0.001$). Also, patients with M-CTC percentage ≥2% had significantly greater multi-intrahepatic and lung-only recurrence than those with M-CTC percentage <2% (multi-intrahepatic: 50.9% vs. 21.1%, $P = 0.004$; lung only: 47.1% vs. 21.1%, $P = 0.011$; Fig. 2G). In contrast, patients with M-CTC percentage <2% had greater single-intrahepatic recurrence than those with M-CTC percentage ≥2% (28.3% vs. 63.2%, $P = 0.001$).

Dynamic changes in CTC count and subtype following surgery and their prognostic significance

Postoperative CTC levels were measured in all 112 patients at 8–10 days following resection. As shown in Fig. 3A, the total CTC count dropped dramatically after surgery, as did the count of each subtype. The proportion of epithelial CTCs and each type of hybrid CTC also dropped. However, the M-CTC percentage increased (Fig. 3B). In addition, there were significant differences of CTC count ($P < 0.001$) and M-CTC percentage ($P = 0.048$) before and 8 to 10 days after surgery in all patients (Fig. 3C and D). However, log-rank tests showed the tumor-free survival rate was significantly associated with changes in M-CTC percentage ($P = 0.033$; Fig. 3E), but not with total CTC count ($P = 0.074$; Fig. 3F). Postoperative CTC monitoring in 10 patients found that 8 had an increased CTC count 1 to 2 months before detectable recurrence or the appearance of metastatic lesions; 6 patients also had increased M-CTC percentage (Fig. 3G; Supplementary Fig. S2).

Differential gene expression profiles in the HCCs with high and low levels of CTCs

To better understand the molecular mechanisms that may contribute to the occurrence of CTCs, the gene expression profiles of 25 patients with typical HCC were analyzed, including 15 patients who had a very high CTC count (≥21) and M-CTC percentage (≥5%), and 10 who had a very low CTC count (≤5) and M-CTC percentage (0%; Fig. 4A). A subset of common

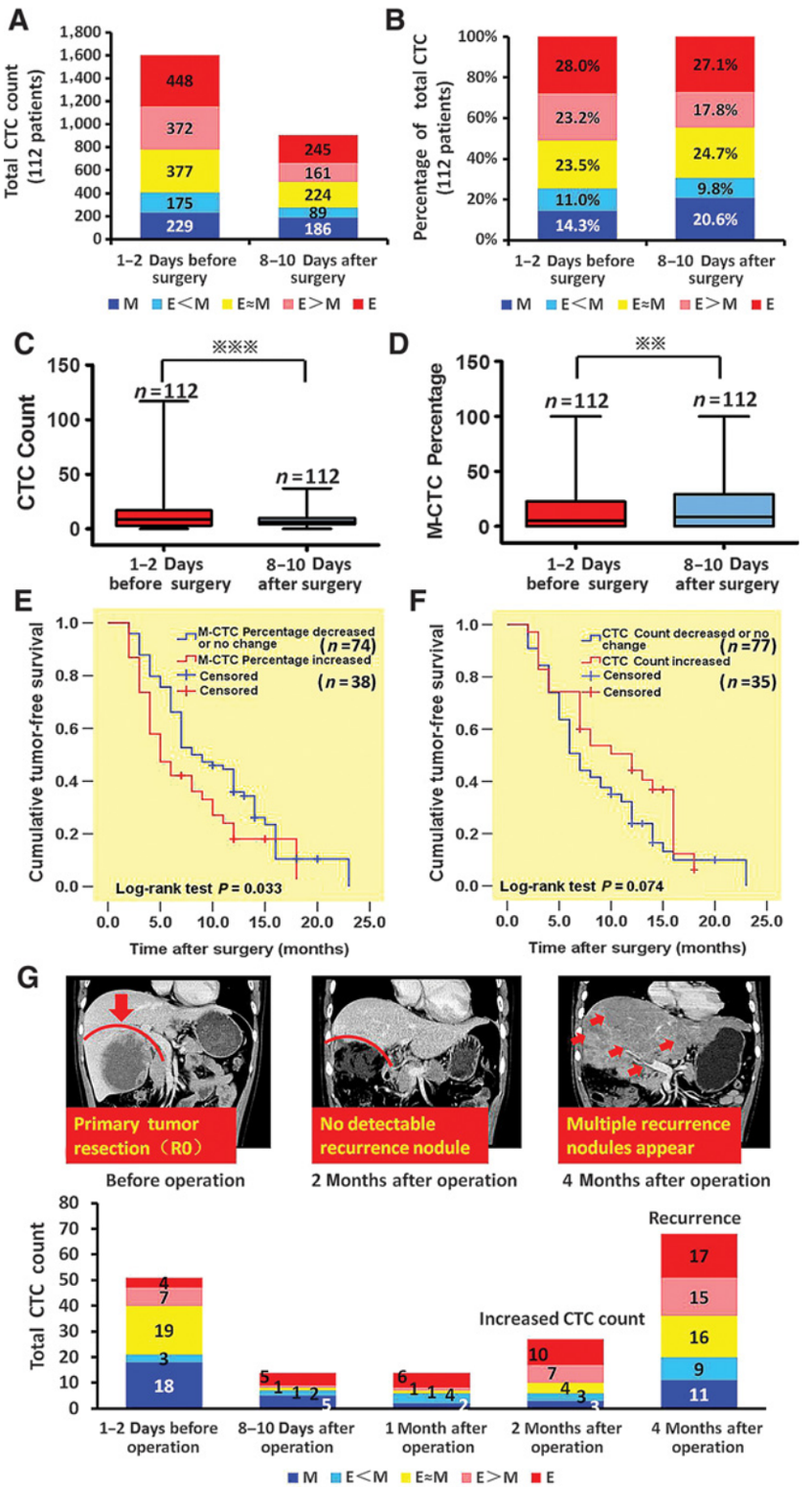

Figure 3.

Analysis of postoperative CTC levels at follow-up. **A** and **B,** Total (**A**) and percentage (**B**) of total CTCs by subtype following surgical resection. **C** and **D,** CTC count (**C**) and M-CTC percentage (**D**) in 112 patients before and 8 to 10 days after surgery. **, $P < 0.05$; ***, $P < 0.001$. **E** and **F,** Postoperative tumor-free survival time by change in CTC count (**E**) or M-CTC percentage (**F**). **G,** Top, Representative CT data from a patient (before surgery and at 2 and 4 months follow-up) who had multi-intrahepatic recurrence at 4 months postoperative follow-up. Bottom, cumulative total CTC count by CTC type before and after surgical resection. At 2 months follow-up (i.e., 2 months before detection of recurrence), this patient's CTC count started to increase.

differentially expressed genes was selected by initial filtering at $P < 0.05$, followed by filtering by expression level (≥2-fold). Using these stringent selection criteria, we found 187 genes were upregulated, and 57 genes were downregulated in HCCs with a high CTC count and M-CTC percentage. Using the ClusterProfiler Package (R/bioconductor; http://www.bioconductor.org/), Kyoto Encyclopedia of Genes and Genomes (KEGG) pathway enrichment analysis showed that 10 KEGG pathways clusters were

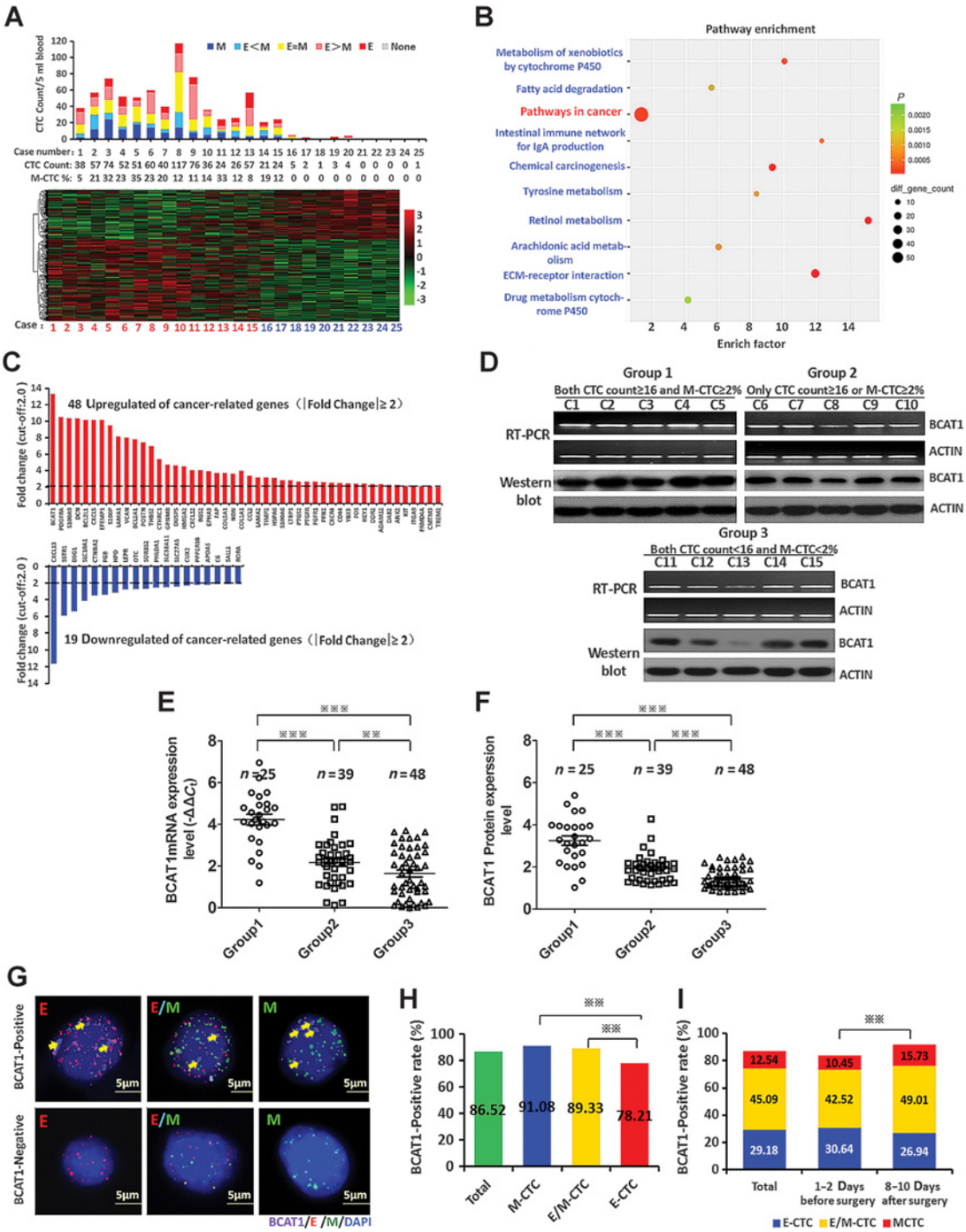

Figure 4.

Gene expression profiles of differentially expressed genes in HCCs that have a high CTC count and M-CTC percentage and validation of BCAT1 gene expression levels in HCCs and CTCs. **A,** Quantitation of EMT features in the CTCs of 25 patients with HCC and hierarchical clustering revealed differentially expressed genes in 15 HCCs (C1–C15), which have a high CTC count and M-CTC percentage, and 10 HCCs (C16–C25), which have a low high CTC count and M-CTC percentage. The level of up- and downregulation is represented by the intensity of the red and green colors, respectively. **B,** KEGG pathway enrichment analysis showed that 10 KEGG pathway clusters were enriched. The "Pathways in cancer" is ranked the first with regard to the differentially expressed gene count. **C,** Sixty-seven cancer-related genes (48 upregulated and 19 downregulated) for which expression levels were ≥2-fold are shown. Among them, one of the identified genes, BCAT1, was significantly upregulated (13.31-fold; $P < 0.05$). **D,** Representative RT-PCR and Western blot images showing BCAT1 mRNA and protein levels in the following three groups: group 1, CTC count ≥ 16 and M-CTC percentage ≥2% (C1–C5); group 2, CTC count ≥16 or M-CTC percentage ≥2% (C6–C10); and group 3, CTC count <16 and M-CTC percentage <2% (C11–C15). **E** and **F,** qPCR ($-\Delta\Delta$Ct; **E**) and Western blot (**F**) analysis was used to determine mean BCAT1 mRNA and protein expression levels, respectively, for the three subgroups. β-Actin was used as an internal control. **, $P < 0.05$; ***, $P < 0.001$. **G,** RNA-ISH analysis of BCAT1 expression in each CTC subtype. **H,** The BCAT1-positive rate in the total CTCs, epithelial CTCs (E-CTC), epithelial/mesenchymal hybrid CTCs (E/M-CTC), and mesenchymal CTCs (M-CTC).**, $P < 0.05$; ***, $P < 0.001$. **I,** The BCAT1-positive rate in CTCs 1–2 days before surgery and 8–10 days after surgery. **, $P < 0.05$; ***, $P < 0.001$.

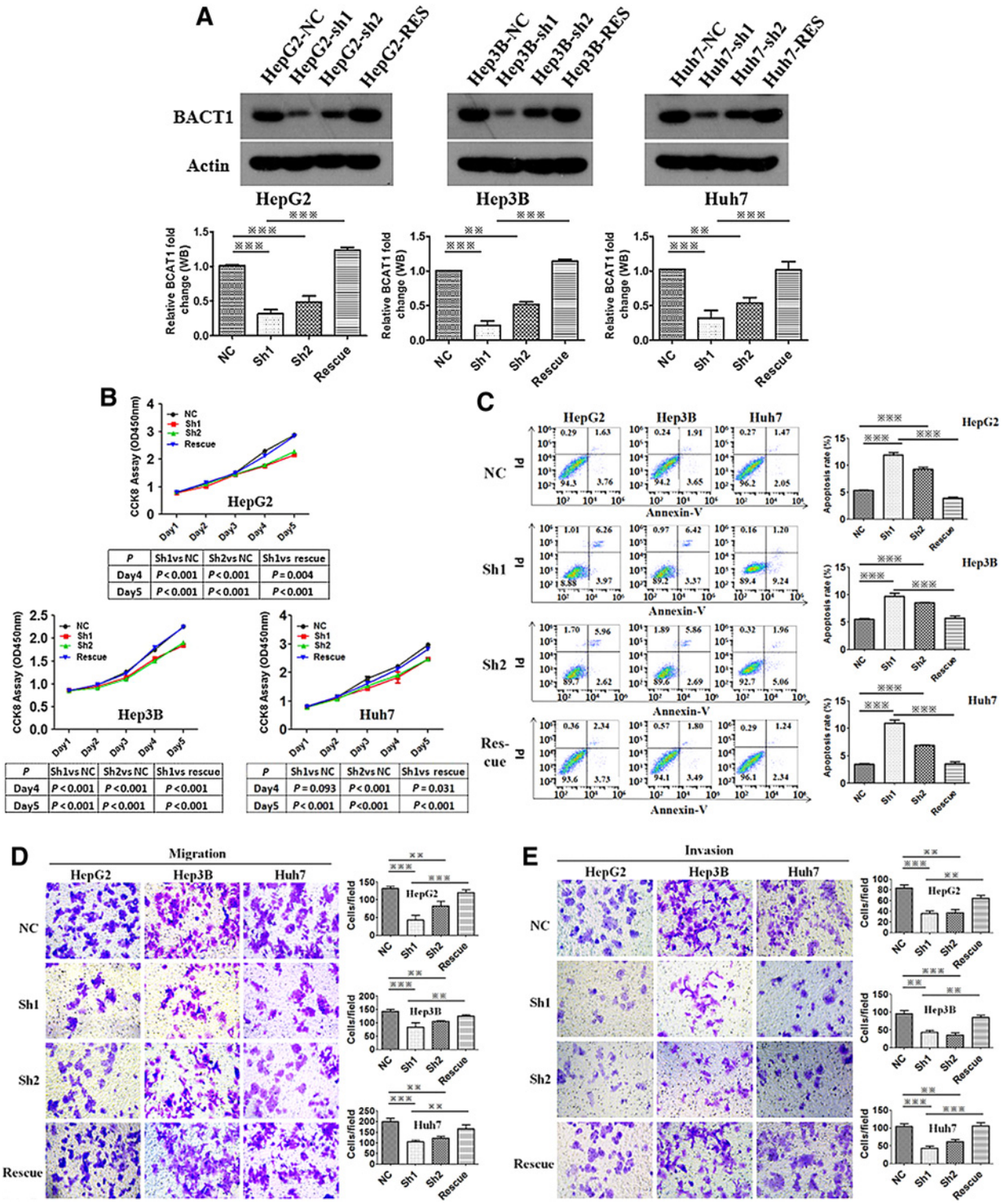

Figure 5.

Knockdown of BCAT1 induces cell apoptosis and reduces cell proliferation, migration, and invasion. **A,** Western blot validation of BCAT1 protein knockdown and rescue in selected clones (sh-1, sh-2, and sh1-rescue) and NC controls; **, $P < 0.05$; ***, $P < 0.001$ ($n = 3$). **B,** Cell proliferation was evaluated at the indicated time points using the CCK8 assay ($n = 3$). **C,** Cell apoptosis was measured by flow cytometric analysis. **, $P < 0.05$; ***, $P < 0.001$ ($n = 3$). **D** and **E,** Migration (**D**) and invasion (**E**) of cells using Transwell chambers and Matrigel-coated invasion chambers, respectively. **, $P < 0.05$; ***, $P < 0.001$ ($n = 3$).

enriched (Fig. 4B). We found "Pathways in cancer" is ranked the first with regard to differentially expressed gene count; this pathway includes nine important canonical cancer pathways, such as the Wnt, FAK, and PI3K–AKT signaling pathways (Supplementary Fig. S3). In total, 67 cancer-related genes (48 upregulated and 19 downregulated) were differentially expressed (Fig. 4C). Using Ingenuity Pathway Analysis (IPA; http://www.Ingenuity.com) to classify the biological processes that may be affected by the 67 cancer-related genes, we showed that they take part in seven cancer-related biological processes (e.g., cell adhesion and migration, tumor angiogenesis, and apoptosis; Supplementary Table S5).

One of the 67 differentially cancer-related genes identified was BCAT1, which was significantly upregulated (13.31-fold, $P < 0.05$; Fig. 4C). BCAT1 upregulation was confirmed by RT-PCR, qPCR, and Western blot analysis in 112 samples, which were categorized into three groups: group 1 (CTC count $\geq$16 and M-CTC percentage $\geq$2%, $n = 25$), group 2 (CTC count $\geq$16 or M-CTC percentage$\geq$2%, $n = 39$), and group 3 (CTC count <16 and M-CTC percentage <2%, $n = 48$). Representative examples of RT-PCR and Western blot were shown in Fig. 4D. We found the mRNA ($-\Delta\Delta Ct$: by qPCR) and protein expression levels of BACT1 were significantly different among the three groups (Fig. 4E and F). In addition, BCAT1 was also validated by RNA-ISH in CTCs from 79 of 112 patients (Fig. 4G); it was detected in 1,778 of 2,055 (86.52%) CTCs analyzed. The BCAT1-positive rate was significantly higher in M-CTCs and E/M-CTCs compared with E-CTCs (91.08% and 89.33% vs.78.21%, respectively; $P < 0.05$; Fig. 4H). Furthermore, the BCAT1-positive rate was also significantly increased 8 to 10 days after surgery as compared with that before surgery (91.68% vs. 83.61%, $P < 0.05$; Fig. 4I).

Overexpression of BCAT1 induces HCC proliferation, migration, and invasion and reduces apoptosis, possibly by triggering EMT

We next analyzed the impact of BCAT1 knockdown on HCC proliferation, apoptosis, migration, and invasion in the Hepg2, Hep3B, and Huh7 cell lines, which displayed moderate-to-strong BCAT1 expression (data not shown). As shown in Fig. 5A, the shRNA-BCAT1 knockdown clones (sh-1 and sh-2) displayed decreased BCAT1 expression compared with the NC controls. In addition, BCAT1 expression was efficiently rescued in the RES groups. Thus, these cells were selected for further analyses.

Downregulation of BCAT1 significantly inhibited Hepg2, Hep3B, and Huh7 cell proliferation (Fig. 5B). In addition, the proportion of annexin V–positive cells was significantly higher in both shBCAT groups as compared with the controls (Fig. 5C). Furthermore, BCAT1-sh1 and BCAT1-sh2 cells had decreased migration and invasion as compared with controls (Fig. 5D and E). Importantly, these effects were ameliorated with BCAT1-sh1-rescue (Fig. 5B–E).

We also examined whether the downregulation of BCAT1 could impact EMT in HCC cells. qPCR analysis showed that E-cadherin mRNA level was significantly increased in both shBCAT1 groups as compared with the controls (Fig. 6A). EpCAM mRNA levels were also increased in the sh1BCAT1 groups, as well as in the sh2BCAT1 groups of HepG2 and Huh7 cells (Fig. 6A). Conversely, expression of mesenchymal markers mRNA (vimentin and Twist) was significantly decreased in both shBCAT1 groups as compared with controls (Fig. 6B). Similar results were found using Western blot analysis to evaluate protein levels of the cellular markers (Fig. 6C–E). Taken together, upregulation of BCAT1 enhances cell proliferation, migration, and invasion; BCAT1 overexpression also likely triggers the EMT process.

Discussion

Because the presence of CTCs is reflective of the aggressiveness of a solid tumor, many attempts have been made to develop assays that reliably detect and enumerate these cells. Although the Cellsearch System has been used in the majority of published studies, it depends on tumor epithelial cell expression of EpCAM, the presence of an intact nucleus, and the absence of CD45 (4, 7, 25–31). However, this approach may fail to detect the CTCs undergoing EMT (e.g., mesenchymal-like CTCs). Thus, we used CanPatrol CTC enrichment that detects a combination of epithelial and mesenchymal markers.

CTCs were detected in 90.18% of patients with HCC, and in more than half of patients with early-stage HCC (BCLC 0–A stage), suggesting that tumor dissemination may be an early event in HCC pathogenesis. We also unexpectedly detected low levels of CTCs in two of 12 patients with HBV, and both developed CT/MRI-detectable small HCC tumors during the subsequent 5 months. This was consistent with a report suggesting metastasis may occur long before the primary tumor is detectable (32). CTCs were detected in a small fraction of patients with chronic obstructive pulmonary disease, and the annual surveillance of these CTC-positive patients by CT-scan screening detected lung nodules 1 to 4 years after CTC detection, leading to diagnosis of early-stage lung cancer (33). Because HBV infection can eventually result in HCC (1, 34–36), detection of CTCs in these patients may represent a marker of undetectable, very early-stage disease. Thus, for patients with high risk of developing HCC (e.g., those with HBV infection or hepatic cirrhosis), CTC examination may be an important tool to detect minimal liver cancer at an extremely early stage. Further studies will assess the diagnostic value of this potential tool for detecting liver cancer at early stages in high-risk populations.

HCC recurrence is an important factor for prognosis, although the recurrence time interval and mode varies (37). Hybrid CTCs might be a vital factor for intrahepatic metastasis, while M-CTCs may predict extrahepatic metastasis (17). In this study, multivariate analyses revealed that total CTC count and M-CTC percentage were factors for postoperative HCC recurrence, and ROC analysis indicated a CTC count of 16 and M-CTC percentage of 2% had the best sensitivity and specificity for predicting recurrence within 6 months following resection. Moreover, the multi-intrahepatic recurrence rate and lung metastasis rate were significantly higher in patients with CTC count $\geq$16 or M-CTC percentage $\geq$2%, suggesting that multi-intrahepatic recurrence and lung metastasis may represent CTC-induced recurrence. Therefore, CTC count $\geq$16 or M-CTC percentage $\geq$2% preoperatively may predict early recurrence, and the type of recurrence (i.e., multi-intrahepatic recurrence and/or lung metastasis). Apart from the presence of CTCs, there are several risk factors that may contribute to single-intrahepatic HCC recurrence, such as liver cirrhosis or HBV reactivation. Studies indicate most delayed tumor recurrences after curative therapy may not be metastasis from the original tumor, but rather *de novo* cancers arising in a cirrhotic liver or as a result of HBV reactivation (1, 38). This is consistent with the present study that found single-intrahepatic recurrence accounted for the majority of delayed tumor recurrences.

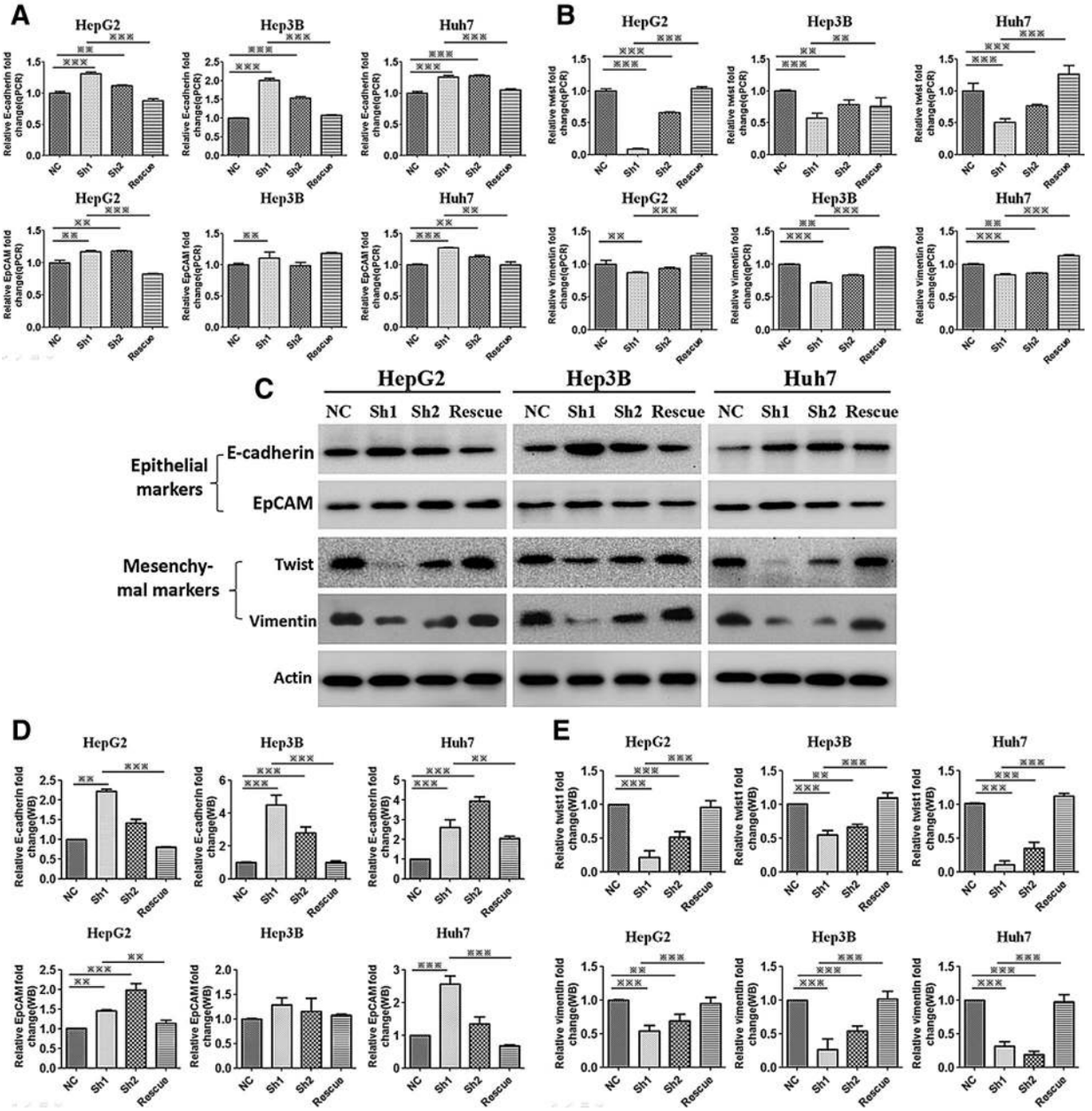

Figure 6.

Knockdown of BCAT1 inhibits the EMT. **A** and **B,** The expression of epithelial markers mRNA (EpCAM and E-cadherin; **A**) and mesenchymal markers mRNA (vimentin and Twist; **B**) were validated by qPCR. **, $P < 0.05$; ***, $P < 0.001$ ($n = 3$). **C,** Representative Western blot images showed the similar results in terms of the protein levels of epithelial markers (EpCAM and E-cadherin) and mesenchymal markers (vimentin and Twist) compared with qPCR ($n = 3$). **D** and **E,** The expression protein levels of epithelial markers (EpCAM and E-cadherin; **D**) and mesenchymal markers (vimentin and Twist; **E**) among the BCAT1 knockdown (sh-1 and sh-2) and control (NC and sh1-rescue) groups as determined by Western blot analysis. **, $P < 0.05$; ***, $P < 0.001$ ($n = 3$).

The clinical use of monitoring CTC changes with treatment has been reported in other types of cancers. A significant decrease in CTC load was observed soon after curative HCC resection, which may be attributed to surgical resection of the primary tumor, and patients whose CTC count failed to drop to <2 postoperatively showed a propensity toward increased recurrence (7). In contrast, there was no significant association between changes in CTC count and recurrence rate and time to recurrence in our study, although more than half of the patients had decreased CTC count immediately following resection. Although the reason for this observation is unknown, mechanical extrusion of the tumor during resection may have caused tumor cells to be released into the blood, thereby increasing the early postoperative CTC count. It is possible that these CTCs may lack the ability to survive, and thus

do not result in early recurrence. Therefore, early postoperative changes in CTC levels cannot accurately represent the efficacy of surgery. However, patients who had an increased M-CTC percentage showed a propensity toward increased recurrence and a relatively short disease-free survival period, which may be attributed to BCAT1 overexpression.

We also monitored postoperative CTC changes in 10 patients and found that most had increased CTCs 1 to 2 months before clinically detectable recurrence nodules appeared. However, it is not clear what caused the increased CTC levels, as CTC self-proliferation in blood following dissemination from the primary tumor has not been reported. The presence of CTCs may be associated with actively proliferating metastases elsewhere, even undetectable metastases (32). As we previously mentioned, tumor dissemination may be an early event in HCC progression; therefore, metastatic lesions may release tumor cells into the blood circulation even before they are detectable (32, 37). Thus, postoperative monitoring of CTC changes may provide an earlier predictor of recurrence compared with conventional imaging (e.g., ultrasonography and CT).

Gene expression profile analysis of HCCs with very high CTC levels, and those with very low CTC levels revealed the "Pathways in cancer" was ranked first with regard to differentially expressed genes. In total, 67 cancer-related genes were identified that play an important part in seven cancer-related biological processes, some of which were metastasis-related biological process (e.g., positive regulation of cell invasion and migration, tumor angiogenesis, and negative regulation of apoptosis). We observed that most genes involved in these metastasis-related biological processes were upregulated. In contrast, genes that positively regulate apoptosis were downregulated (e.g., *DSG1*, *SLC38A11*, and *SLC10A1*). Thus, some compensatory dissemination/metastasis mechanisms may exist in HCCs, which may result in high CTC count and M-CTC percentage.

BCAT1 was one of 67 differentially cancer-related genes identified and was significantly upregulated in HCCs with high CTC count and M-CTC percentage. Also, the positive rate for BCAT1 expression in CTCs was 86.52%, and 91.08% of M-CTCs were positive for BCAT1 expression. BCAT1 is located at 12p12.1, and codes for a transaminase that catalyzes the reversible transamination of branched-chain alpha-keto acids to branched-chain L-amino acids essential for cell growth (39, 40). Studies have confirmed that BCAT1 is involved in cell proliferation, differentiation, and apoptosis and plays an important role in several malignancies, especially in the progression of nonseminomas (41–43). We showed that Hepg2, Hep3B, and Huh7 cell migration and invasion were reduced with BCAT1 knockdown, which may be due to inhibition of EMT as observed by increased expression of epithelial markers (EpCAM and E-cadherin), and reduced expression of mesenchymal markers (vimentin and Twist). In addition, BCAT1 knockdown significantly inhibited cell proliferation and promoted apoptosis. Thus, overexpression of BCAT1 in CTCs may increase their invasive potential and their resistance to apoptosis. Given that patients with a high M-CTC percentage before surgery, and those with increased M-CTC percentage after surgery had significantly shorter time to recurrence, it is possible that this is related to BCAT1 expression as a large proportion of M-CTCs were positive for BCAT1.

EpCAM is considered a cancer stem cell marker (44), and EpCAM-positive CTCs with stem cell–like phenotypes might also represent a more aggressive subset of CTCs, which lead to local recurrence or distant metastasis (7). The reason several patients who had predominantly E-CTCs, especially those with relatively higher CTC count ($\geq$16), had a shorter time to recurrence may be because some E-CTCs or E/M hybrid CTCs may be EpCAM-positive CTCs.

Our results do not allow us to draw a definitive conclusion if there is a correlation between a high CTC count and a specific CTC subpopulation ratio. However, there are a number of reasons for the correlation between high CTC count and shorter tumor-free time. First, patients with high CTC count are likely to have high M-CTC percentages, and M-CTCs are regarded as the most malignant CTC. Similarly, patients with higher CTC counts, especially E-CTC-dominant patients, may also have a higher proportion of EpCAM-positive CTCs. As mentioned above, EpCAM-positive CTCs may also represent a more aggressive subset of CTCs. Finally, theoretically, the higher CTC count, the higher the chance of recurrence/metastasis. Therefore, patients with high numbers of CTCs, even those without a higher M-CTC or EpCAM-positive CTC percentage, may also have a greater chance of early recurrence.

There are some limitations of this study. Tumor cells often show a wide range of sizes. Because the CanPatrol system is filtration-based device, the detection efficiency may be biased in that small CTCs could easily cross the barriers. To overcome this potential limitation, multi-CTC detection techniques may be used in further studies to improve the detection efficiency. In addition, this study focused only on the relation between BCAT1 overexpression and CTC release.

Conclusions

The majority of patients with HCC had CTCs, even those with early-stage HCC. CTC count $\geq$16 and M-CTC percentage $\geq$2% prior to resection was a predictor of early recurrence and was associated with multi-intrahepatic recurrence and lung metastasis. Postoperative monitoring of CTC levels may predict HCC recurrence before clinically detectable recurrence nodules appear. Many metastasis-related genes and biological pathways may contribute to CTCs. Suppression of BCAT1 reduced HCC cell proliferation, migration, and invasion and promoted apoptosis likely by inhibiting EMT. Taken together, our study provides additional insights into the clinical significance and the mechanisms of CTCs in HCC.

Disclosure of Potential Conflicts of Interest

No potential conflicts of interest were disclosed.

Authors' Contributions

Conception and design: L.-N. Qi, B.-D. Xiang, L.-Q. Li
Development of methodology: B.-D. Xiang, L.-Q. Li
Acquisition of data (provided animals, acquired and managed patients, provided facilities, etc.): J.-Z. Ye, J.-H. Zhong, Z.-S. Chen
Analysis and interpretation of data (e.g., statistical analysis, biostatistics, computational analysis): J.-H. Zhong, Y.-Y. Chen
Writing, review, and/or revision of the manuscript: L.-N. Qi
Administrative, technical, or material support (i.e., reporting or organizing data, constructing databases): F.-X. Wu, Y.-Y. Wang, L. Ma, J. Chen, W.-F. Gong, Z.-G. Han, Y. Lu, J.-J. Shang
Study supervision: L.-N. Qi, F.-X. Wu, L. Ma, L.-Q. Li

Acknowledgments

This work was supported by the National Nature Science Foundation of China (NSFC 81502533, 81260088, 81160262, 81260331) and Guangxi

Nature Sciences grants (2013GXNSFBA019196, Gui Ke AB16380242). This work was also supported in part by the Guangxi Medical University Training Program for Distinguished Young Scholars.

The costs of publication of this article were defrayed in part by the payment of page charges. This article must therefore be hereby marked *advertisement* in accordance with 18 U.S.C. Section 1734 solely to indicate this fact.

Received August 20, 2017; revised March 21, 2018; accepted June 12, 2018; published first June 18, 2018.

References

1. Bruix J, Gores GJ, Mazzaferro V. Hepatocellular carcinoma: clinical frontiers and perspectives. Gut 2014;63:844–55.
2. Bruix J, Reig M, Sherman M. Evidence-based diagnosis, staging, and treatment of patients with hepatocellular carcinoma. Gastroenterology 2016;150:835–53.
3. Alix-Panabieres C, Pantel K. Challenges in circulating tumour cell research. Nat Rev Cancer 2014;14:623–31.
4. Hou JM, Krebs M, Ward T, Sloane R, Priest L, Hughes A, et al. Circulating tumor cells as a window on metastasis biology in lung cancer. Am J Pathol 2011;178:989–96.
5. Lohr JG, Adalsteinsson VA, Cibulskis K, Choudhury AD, Rosenberg M, Cruz-Gordillo P, et al. Whole-exome sequencing of circulating tumor cells provides a window into metastatic prostate cancer. Nat Biotechnol 2014;32:479–84.
6. Sun W, Li G, Wan J, Zhu J, Shen W, Zhang Z. Circulating tumor cells: A promising marker of predicting tumor response in rectal cancer patients receiving neoadjuvant chemo-radiation therapy. Oncotarget 2016;7: 69507–17.
7. Sun YF, Xu Y, Yang XR, Guo W, Zhang X, Qiu SJ, et al. Circulating stem cell-like epithelial cell adhesion molecule-positive tumor cells indicate poor prognosis of hepatocellular carcinoma after curative resection. Hepatology 2013;57:1458–68.
8. Yu M, Bardia A, Wittner BS, Stott SL, Smas ME, Ting DT, et al. Circulating breast tumor cells exhibit dynamic changes in epithelial and mesenchymal composition. Science 2013;339:580–4.
9. Lu J, Fan T, Zhao Q, Zeng W, Zaslavsky E, Chen JJ, et al. Isolation of circulating epithelial and tumor progenitor cells with an invasive phenotype from breast cancer patients. Int J Cancer 2010;126:669–83.
10. von Felden J, Schulze K, Krech T, Ewald F, Nashan B, Pantel K, et al. Circulating tumor cells as liquid biomarker for high HCC recurrence risk after curative liver resection. Oncotarget 2017;8:89978–87.
11. Guarino M. Epithelial–mesenchymal transition and tumour invasion. Int J Biochem Cell Biol 2007;39:2153–60.
12. Ksiazkiewicz M, Markiewicz A, Zaczek AJ. Epithelial–mesenchymal transition: a hallmark in metastasis formation linking circulating tumor cells and cancer stem cells. Pathobiology 2012;79:195–208.
13. Pantel K, Brakenhoff RH. Dissecting the metastatic cascade. Nat Rev Cancer 2004;4:448–56.
14. Nel I, Baba HA, Ertle J, Weber F, Sitek B, Eisenacher M, et al. Individual profiling of circulating tumor cell composition and therapeutic outcome in patients with hepatocellular carcinoma. Transl Oncol 2013;6:420–8.
15. Li Y, Zhang X, Ge S, Gao J, Gong J, Lu M, et al. Clinical significance of phenotyping and karyotyping of circulating tumor cells in patients with advanced gastric cancer. Oncotarget 2014;5:6594–602.
16. Schramm A, Mueller V, Huober J. P176 The DETECT study concept-circulating tumor cells (CTCs) in metastatic breast cancer. Breast 2015;24: 85–6.
17. Liu YK, Hu BS, Li ZL, He X, Li Y, Lu LG. An improved strategy to detect the epithelial–mesenchymal transition process in circulating tumor cells in hepatocellular carcinoma patients. Hepatol Int 2016;10:640–6.
18. Si Y, Lan G, Deng Z, Wang Y, Lu Y, Qin Y, et al. Distribution and clinical significance of circulating tumor cells in nasopharyngeal carcinoma. Jpn J Clin Oncol 2016;46:622–30.
19. Wu S, Liu S, Liu Z, Huang J, Pu X, Li J, et al. Classification of circulating tumor cells by epithelial–mesenchymal transition markers. PLoS One 2015;10:e0123976.
20. Wu S, Liu Z, Liu S, Lin L, Yang W, Xu J. Enrichment and enumeration of circulating tumor cells by efficient depletion of leukocyte fractions. Clin Chem Lab Med 2015;53:337.
21. The International Agency for Research on Cancer. WHO classification of tumours of the digestive system (IARC WHO classification of tumours). 4th ed. In:Bosman FT, Carneiro F, Hruban RH, Theise ND, editors: World Health Organization; 2010. P.1–418.
22. Bruix J, Sherman M; American Association for the Study of Liver Disease. Management of hepatocellular carcinoma: an update. Hepatology 2011; 53:1020–2.
23. Li TT, Liu H, Li FP, Hu YF, Mou TY, Lin T, et al. Evaluation of epithelial–mesenchymal transitioned circulating tumor cells in patients with resectable gastric cancer: Relevance to therapy response. World J Gastroenterol 2015;21:13259–67.
24. Zhao R, Cai Z, Li S, Cheng Y, Gao H, Liu F, et al. Expression and clinical relevance of epithelial and mesenchymal markers in circulating tumor cells from colorectal cancer. Oncotarget 2017;8: 9293–302.
25. Allard WJ, Matera J, Miller MC, Repollet M, Connelly MC, Rao C, et al. Tumor cells circulate in the peripheral blood of all major carcinomas but not in healthy subjects or patients with nonmalignant diseases. Clin Cancer Res 2004;10:6897–904.
26. Chang K, Kong YY, Dai B, Ye DW, Qu YY, Wang Y, et al. Combination of circulating tumor cell enumeration and tumor marker detection in predicting prognosis and treatment effect in metastatic castration-resistant prostate cancer. Oncotarget 2015;6:41825–36.
27. Guo W, Yang XR, Sun YF, Shen MN, Ma XL, Wu J, et al. Clinical significance of EpCAM mRNA-positive circulating tumor cells in hepatocellular carcinoma by an optimized negative enrichment and qRT-PCR-based platform. Clin Cancer Res 2014;20:4794–805.
28. Janni WJ, Rack B, Terstappen LW, Pierga JY, Taran FA, Fehm T, et al. Pooled analysis of the prognostic relevance of circulating tumor cells in primary breast cancer. Clin Cancer Res 2016;22:2583–93.
29. Kelley RK, Magbanua MJ, Butler TM, Collisson EA, Hwang J, Sidiropoulos N, et al. Circulating tumor cells in hepatocellular carcinoma: a pilot study of detection, enumeration, and next-generation sequencing in cases and controls. BMC Cancer 2015;15:206.
30. Riethdorf S, Fritsche H, Muller V, Rau T, Schindlbeck C, Rack B, et al. Detection of circulating tumor cells in peripheral blood of patients with metastatic breast cancer: a validation study of the CellSearch system. Clin Cancer Res 2007;13:920–8.
31. Tu Q, Wu X, Le Rhun E, Blonski M, Wittwer B, Taillandier L, et al. CellSearch technology applied to the detection and quantification of tumor cells in CSF of patients with lung cancer leptomeningeal metastasis. Lung Cancer 2015;90:352–7.
32. Klein CA. Parallel progression of primary tumours and metastases. Nat Rev Cancer 2009;9:302–12.
33. Ilie M, Hofman V, Long-Mira E, Selva E, Vignaud JM, Padovani B, et al. "Sentinel" circulating tumor cells allow early diagnosis of lung cancer in patients with chronic obstructive pulmonary disease. PLoS One 2014;9: e111597.
34. Gao J, Xie L, Yang WS, Zhang W, Gao S, Wang J, et al. Risk factors of hepatocellular carcinoma–current status and perspectives. Asian Pac J Cancer Prev 2012;13:743–52.
35. Ortiz-Cuaran S, Villar S, Gouas D, Ferro G, Plymoth A, Khuhaprema T, et al. Association between HBX status, aflatoxin-induced R249S TP53 mutation and risk of hepatocellular carcinoma in a case-control study from Thailand. Cancer Lett 2013;331:46–51.
36. Qi LN, Bai T, Chen ZS, Wu FX, Chen YY, De Xiang B, et al. The p53 mutation spectrum in hepatocellular carcinoma from Guangxi, China: role of chronic hepatitis B virus infection and aflatoxin B1 exposure. Liver Int 2015;35:999–1009.
37. Nguyen DX, Bos PD, Massague J. Metastasis: from dissemination to organ-specific colonization. Nat Rev Cancer 2009;9:274–84.
38. Llovet JM, Bruix J. Novel advancements in the management of hepatocellular carcinoma in 2008. J Hepatol 2008;48:S20–37.

39. Eden A, Simchen G, Benvenisty N. Two yeast homologs of ECA39, a target for c-Myc regulation, code for cytosolic and mitochondrial branched-chain amino acid aminotransferases. J Biol Chem 1996;271:20242–5.
40. Schuldiner O, Eden A, Ben-Yosef T, Yanuka O, Simchen G, Benvenisty N. ECA39, a conserved gene regulated by c-Myc in mice, is involved in G1/S cell cycle regulation in yeast. Proc Natl Acad Sci U S A 1996;93:7143–8.
41. Mayers JR, Torrence ME, Danai LV, Papagiannakopoulos T, Davidson SM, Bauer MR, et al. Tissue of origin dictates branched-chain amino acid metabolism in mutant Kras-driven cancers. Science 2016;353:1161–5.
42. Wang ZQ, Faddaoui A, Bachvarova M, Plante M, Gregoire J, Renaud MC, et al. BCAT1 expression associates with ovarian cancer progression: possible implications in altered disease metabolism. Oncotarget 2015;6:31522–43.
43. Zhou W, Feng X, Ren C, Jiang X, Liu W, Huang W, et al. Over-expression of BCAT1, a c-Myc target gene, induces cell proliferation, migration and invasion in nasopharyngeal carcinoma. Mol Cancer 2013;12:53.
44. Terris B, Cavard C, Perret C. EpCAM, a new marker for cancer stem cells in hepatocellular carcinoma. J Hepatol 2010;52:280–1.